Advances in Aerospace Science and Applications.
ISSN 2277-3223 Volume 3, Number 2 (2013), pp. 35-46

http://www.ripublication.com/aasa.htm

Velocity Perturbations Analysis of the Fengyun-1C Satellite Fragmentation Event

Arjun Tan and Mark Dokhanian

Department of Physics, Alabama A & M University
P.O. Box 447, Normal, AL 35762, U. S. A.
E-mail: arjun.tan@aamu.edu

Abstract

The anti-satellite (ASAT) experiment conducted by the People's Republic of China on its own Fengyun-1C weather satellite in 2007 created the largest amount of orbital debris in the history of satellite fragmentation. This event is analyzed by studying the velocity perturbations analysis of 2,141 fragments cataloged through 201 days following the event in three orthogonal (radial, down-range and cross-range) directions in the parent satellite's frame of reference. The first 503 fragments cataloged through day 17 following the breakup exhibited the perfect Gabbard diagram and were therefore subjected to further detailed analysis. The histograms of the velocity perturbations components in all three directions generally showed Gaussian patterns displaced from the origins, which bear signs of external impact. Two-dimensional scatter-plots in the horizontal and two vertical planes show high asymmetries in the distributions of the fragments indicative of the probable direction of the ASAT. A three-dimensional scatter-plot of the same provides a bird's eye view of the dispersion of the fragments. Fragment counts in eight octants of space in the parent's frame of reference give further details of the fragments spread and reinforce the probable direction of the oncoming ASAT. Finally, the similarities and differences between this experiment and the U.S. ASAT test against Solwind P78-1 satellite 22 years earlier are discussed.

INTRODUCTION

On 11 January 2007, the People's Republic of China conducted its anti-satellite (ASAT) test [1]. The target was its own weather satellite Fengyun-1C (International designator 1999-025A; U.S. satellite catalog number 25730), which had been in operation since its launch on 10 May 1999 into a near-circular Sun-synchronous orbit [2]. The ASAT was a kinetic kill-vehicle launched from a mobile transporter-erector

launcher near the Xichang Space Center aboard a two-stage ballistic missile [3]. The destruction of the satellite occurred at 2226 GMT (epoch 200711.90621003) at latitude 35^{o}N, longitude 100^{o}E and altitude of 860 km [2]. This ASAT test was reminiscent of the U.S. ASAT experiment conducted on 13 September 1985 against the Solwind P78-1 satellite [4].

The fragmentation of the Fengyun-1C satellite produced, by far, the largest amount of orbital debris ever recorded [5]. Over 3,000 trackable debris from that event have been cataloged thus far, accounting for well over 50% of all debris recorded [6]. Normally, all trackable debris are discovered and cataloged within 150 days after a breakup [5]. In the case of the Fengyun-1C fragmentation, additional debris were found and cataloged far beyond that date [6]. The U.S. Space Surveillance Network catalogs the orbital elements of each trackable object in orbit, which can be accessed from the www.space-track.org website of the Department of Defense [7]. In this study, we have considered 2,141 fragments of the breakup, which were cataloged through day 212 of 2007 (201 days following the breakup) and calculated their velocity perturbations (ejection velocities from the parent satellite) from the orbital elements sets. We have used the method prescribed by Badhwar, et al. [8], which has been successfully utilized to analyze the Solwind ASAT experiment [9], Delta 180 collision experiment [10], the Spot 1 Ariane rocket fragmentation [11], and the accidental collision of Iridium 33 and Cosmos 2251 satellites [12].

METHOD OF ANALYSIS

One of the most important quantities in a satellite fragmentation is the velocity change imparted to each fragment. The magnitude, distribution and directionality of the velocity changes are quite indicative of the nature and intensity of the fragmentation. An internal explosion, for example, produces a characteristic beta distribution in fragment velocity changes [8]. A hypervelocity impact by an external object is likely to produce a highly anisotropic distribution of the fragments [9,10]. A glancing impact produces ricochet fragments of unusually high velocity enhancements [13].

It is most convenient to use the parent satellite's frame of reference at the instant of the fragmentation. In a vertical plane, the velocity of the satellite $\vec{v}$ consists of a down-range component v_d and a vertical component v_r . In terms of the gravitational parameter μ, the semi major axis a, eccentricity e and the radial distance from the center of the Earth r, one has:

$$v = \sqrt{\mu\left(\frac{2}{r} - \frac{1}{a}\right)} \tag{1}$$

$$v_d = \frac{1}{r}\sqrt{\mu a(1 - e^2)} \tag{2}$$

and

$$v_r = \pm\frac{1}{a}\sqrt{\mu a e^2 - \frac{\mu}{a}(r - a)^2} \tag{3}$$

In Eq. (3), the + sign corresponds to the ascending mode of the satellite (true anomaly $\nu > \pi$), whereas the – sign corresponds to the descending mode ($\nu < \pi$). The true anomaly ν is obtained from the mean anomaly M via the eccentric anomaly ω:

$$\nu = 2tan^{-1}\left(\sqrt{\frac{1+e}{1-e}}tan\frac{\omega}{2}\right) \tag{4}$$

and

$$\omega \approx M + esinM + \frac{1}{2}e^2sin2M + \frac{1}{8}e^3(3sin3M - sinM) \tag{5}$$

Upon fragmentation, the velocity of a fragment has the components $v_r + dv_r$, $v_d + dv_d$ and dv_x, where the velocity perturbation components of the fragment are in the three orthogonal directions (radial, down-range and cross-range) are given by [8]:

$$dv_r = \pm\sqrt{\mu\left(\frac{2}{r} - \frac{1}{r'}\right) - \frac{\mu a'}{r^2}(1 - e'^2)} - v_r \tag{6}$$

$$dv_d = \frac{cos\zeta}{r}\sqrt{\mu a'(1 - e'^2)} - v_d \tag{7}$$

and

$$dv_x = \frac{sin\zeta}{r}\sqrt{\mu a'(1 - e'^2)} \tag{8}$$

where

$$\zeta = \pm cos^{-1}\frac{cosicosi' + \sqrt{(cos^2\lambda - cos^2 i)(cos^2\lambda - cos^2 i')}}{cos^2\lambda} \tag{9}$$

is the plane change angle of the fragment's orbit from the parent's orbit. In Eqs. (6) – (8), a' is the semi major axis and e' the eccentricity of the fragment's orbit, while in Eq. (9), i and i' are the inclinations of the parent's and fragment's orbits respectively, and λ the latitude of the breakup point. In Eq. (6), the + sign corresponds to the ascending mode of the fragment (true anomaly $\nu' < \pi$), whereas the – sign corresponds to the descending mode ($\nu' > \pi$). In Eq. (9), the + sign corresponds to $i' > i$ and the – sign corresponds to $i' < i$ on the northbound orbits with the opposite sense on the southbound orbits.

The true anomaly ν' of the fragment at the time of the breakup, which dictates the sign of $v_r + dv_r$ in Eq. (6), is determined from the argument of latitude u' and the argument of perigee ω' at the time of fragmentation as

$$\nu' = u' - \omega' \tag{10}$$

The argument of latitude u' is given by

$$u' = sin^{-1}\left(\frac{sin\lambda}{sini'}\right) \tag{11}$$

for northbound motion of the fragment at the time of fragmentation, or by

$$u' = \pi - sin^{-1}\left(\frac{sin\lambda}{sini'}\right) \tag{12}$$

for southbound motion. The argument of perigee of the fragment ω' at the time of breakup t is determined from its value ω'_0 at the time of observation t_0 by [14]:

$$\omega' = \omega'_0 - \frac{4.98\left(5cos^2 i' - 1\right)(t_0 - t)}{\left(a'/r_\oplus\right)^{7/2}(1-e'^2)^2} \tag{13}$$

where $r_\oplus$ is the reference radius of the Earth, ω and ω'_0 are expressed in degrees, and t and t_0 are expressed in days.

THE DATA

Fragments from the Fengyun-1C breakup were continuously tracked and cataloged at unprecedented rates for 201 days, by which time a record 2,141 fragments were officially cataloged [5]. Fragments were still discovered and cataloged after this date, but at far slower rates and after much longer intervals [5]. Orbital elements data collected at later dates normally "age" due to perturbations of various kinds, especially atmospheric drag. Since the Fengyun-1C breakup took place at a relatively higher altitude, drag effects were mainly prominent for fragments with low perigee heights. The orbital elements of the fragments are available at www.space-track.org website of the Department of Defense [2].

In order to uncover the ageing effects of the data, we have separated the 2,141 fragments into six group according to their dates first cataloged as follows: (1) Group I: 503 fragments cataloged between days 4 and 17 after the breakup (13 day period); (2) Group II: 439 fragments cataloged between days 19 and 50 after the breakup (31 day period); (3) Group III: 394 fragments cataloged between days 54 and 85 after the breakup (31 day period); (4) Group IV: 343 fragments cataloged between days 95 and 126 after the breakup (31 day period); (5) Group V: 272 fragments cataloged between days 133 and 166 after the breakup (33 day period); and (6) Group VI: 191 fragments cataloged between days 169 and 201 after the breakup (32 day period).

GABBARD DIAGRAMS

The Gabbard diagram is one of the earliest tools used to study the fragments of a satellite breakup. It plots the heights of apogee and perigee of the fragments against the periods of revolution. The apogee and perigee points lie above and below the inclined "X" on the diagram immediately following the breakup. Atmospheric drag inevitably tends to circularize and move the data points inside the "forbidden zone", especially for the fragments in the lower period region.

Figure 1 shows the Gabbard diagrams for the six groups of the Fengyun-1C fragments cataloged through day 201 after the breakup. The data for the Group I fragments were the most pristine, with no visible points inside the forbidden zone. The velocity perturbations calculated for this group of fragments were, therefore, the most accurate. The Gabbard diagrams for the next groups show progressively greater effects of atmospheric drag, with the arms of the "X" in the lower ends of the period assuming the shapes of "claws" and having points within the claws in addition. For the fragments inside the forbidden zone, the under-root in Eq. (6) becomes imaginary,

thus rendering dv_r imaginary. It is customary to set the under-root equal to zero in order to rescue the dv_r calculation, since the dv_d and dv_x calculations are always reliable.

VELOCITY PERTURBATIONS ANALYSIS

Prior to the impact by the ASAT, Fengyun-1C had an inclination of i = 98.6464°, eccentricity e = .0013513 and mean motion n = 14.11820274, and hence a period of P = 101.996 min [7]. It was in ascending mode (true anomaly ν = 94.0215°). Eqs. (1) – (3) furnish: v = 7.423711 km/s; v_d = 7.423704 km/s; and v_r = 10.005803 m/s. The velocity perturbations of the 2,141 fragments were calculated by Eqs. (6) – (13), as well as the relevant orbital parameters. The values within each group are averaged and entered in Table I. Interestingly, the mean values within the groups were, for the most part, fairly consistent despite the 'ageing' of the data for the later group fragments as portrayed by their Gabbard diagrams. The mean values of dv_r were negative for each group, while the mean values of dv_x were highly negative. The mean values of dv_d, on the other hand, were positive for Groups I and II and negative for the other groups. Since the results were mostly consistent amongst the groups (with the exception of the dv_d values), we shall henceforth restrict our discussion to the Group I fragments only, whose data were the most pristine.

Figure 2 shows the histograms of the velocity perturbations components (dv_d, dv_x and dv_r) of the Group I fragments in the three orthogonal directions in the parent satellite's frame of reference. They were fitted with Gaussian distribution curves centered around the mean values (from Table I). Also shown in the Fig. 2 is the histogram of dv, which was fitted with a Maxwellian type of distribution. Altogether, there were 294 fragments with positive dv_d's and 209 fragments with negative dv_d's. The numbers were quite different in the radial direction: there were 233 fragments with positive dv_r's and 270 fragments with negative dv_r's. However, the figures were the most lop-sided in the cross-range direction: only 96 fragments had positive dv_x's and an astounding 407 fragments had negative dv_x's. This is a clear indication that the ASAT impacted its target from generally the positive cross-range direction. The lack of fragments with high negative values of dv_d's may also suggest that the ASAT struck its target from slightly behind. Similarly, because of the greater number of fragments in the negative radial direction, one might be inclined to infer that the ASAT came from above the horizontal plane.

Figure 3 shows the scatter-plots of the velocity perturbations of the Group I fragments in the horizontal (down-range – cross-range) plane and two vertical planes: one, containing the momentum vector of the parent (radial – down-range plane); and the other containing the orbital angular momentum vector (radial – cross-range plane). The numbers of fragments in each quadrant are marked as well as the probable directions of the oncoming kill vehicle. In the horizontal plane, nearly 48% of the fragments (239 out of 503) were ejected in the fourth quadrant and only 8% (41 out of 503) were ejected in the diametrically opposite second quadrant, which is consistent with the ASAT coming from the latter quadrant. In the vertical $dv_r - dv_x$ plane, 47% (236 out of 503) of the fragments headed in the third quadrant and about 12% (62 out

of 503) were ejected in the diametrically opposite first quadrant. However, the fewest fragments (34 out of 503) were found in the fourth quadrant. Thus the exact direction of the ASAT is inconclusive except that it most likely came from a generally horizontal direction. A more curious observation is found in the $dv_r - dv_d$ plane. Here, the fragments counts were more even in the four quadrants, but the fragments were scattered preferentially in the vertical direction, both upwards and downwards.

Figure 4 is a three-dimensional scatter-plot of the velocity perturbations components of the Group I fragments in the parent's frame of reference in the down-range, cross-range and radial directions, giving a bird's eye-view perspective of the disintegration. Prior to the collision, the direction of the target satellite was nearly along positive dv_d direction. The probable direction of the oncoming ASAT is as shown in the figure. Overall, most of the fragments were bundled on two sides of the ASAT direction consistent with the earlier observation. There appears to be a dearth of fragments opposite the ASAT direction. But there were a handful of fragments ahead along the ASAT direction. One must be mindful that in this three-dimensional plot, many fragments are hidden from the view.

In order to gain a better three-dimensional perspective of the fragmentation, we utilize the three mutually orthogonal axes of dv_d, dv_x and dv_r to define eight octants of space in the parent satellite's frame of reference prior to the fragmentation: (1) Octant I: $dv_d > 0, dv_x > 0, dv_r > 0$; (2) Octant II: $dv_d < 0, dv_x > 0, dv_r > 0$; (3) Octant III: $dv_d < 0, dv_x < 0, dv_r > 0$; (4) Octant IV: $dv_d > 0, dv_x < 0, dv_r > 0$; (5) Octant V: $dv_d > 0, dv_x > 0, dv_r < 0$; (6) Octant VI: $dv_d < 0, dv_x > 0, dv_r < 0$; (7) Octant VII: $dv_d < 0, dv_x < 0, dv_r < 0$; and (8) Octant VIII: $dv_d > 0, dv_x < 0, dv_r < 0$. The numbers of fragments dispersed in each octant are counted and shown in Fig. 5. Nearly 35% of the fragments (175 out of 503) were ejected in Octant VIII alone. This is the octant where the net transfer of momentum must have occurred. However, the fewest fragments were not found in the diametrically opposite Octant II, but in Octant VI below. In spite of this, one would be inclined to assume that the ASAT arrived from Octant II.

The Fengyun-1C fragmentation can be viewed from another angle. The mean values of the velocity perturbation components of the Group I fragments (cf. Table I) define a vector: $\vec{v} = dv_d\hat{x} + dv_x\hat{y} + dv_r\hat{z}$. The magnitude of this vector is $dv = (dv_d^2 + dv_x^2 + dv_r^2)^{1/2}$ = 55.89 m/s. It is not to be confused with dv in Table I, which is the average speed of the individual fragments in a group. The vector $d\vec{v}$ defines two angles relative to the orthogonal coordinate system: (1) the zenith angle $\theta = cos^{-1}(dv_r/dv)$; and (2) the azimuth angle $\phi = tan^{-1}(dv_x/dv_d)$. Upon substituting values, we get θ = 108.47°; and ϕ = −71.52° or 288.48°. Since 90° < θ < 180° and 270° < ϕ < 360°, this places the average direction of the fragments in Octant VIII, the same octant where the largest number of fragments were found. Momentum conservation would dictate that the ASAT must have arrived from the diametrically opposite Octant II. In the frame of reference of the satellite at fragmentation looking vertically downwards, the ASAT came generally from the left; from slightly behind; and from slightly above the horizontal plane. As Fengyun-1C was southbound at location 35°N and 100°E, and the ASAT is believed to have originated at the Xichang Space Center (28°N and 102°E), the direction of the ASAT

is generally in agreement with expectation [15].

A crude estimate of the mass of the ASAT can be made from the momentum analysis. If the masses of the target satellite and the ASAT be M and m respectively, and the relative velocity between the two at collision be V, then, bearing in mind that the debris contained fragments from both objects, one obtains $mV = (M + m)dv$, from which the mass of the ASAT is obtained as $m = Mdv/(V - dv)$. It has been reported that the relative velocity V was 8 km/s [3] and M was 950 kg [2], which yields the mass of the ASAT as m = 6.7 kg. This compares with the ASAT mass in the Solwind fragmentation of 15.9 kg [9]. However, considering the fact that the ASAT contained high-tech guidance and propulsion systems, this value must be considered as an under-estimation.

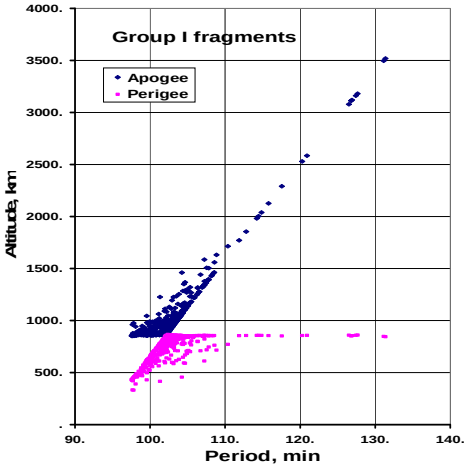

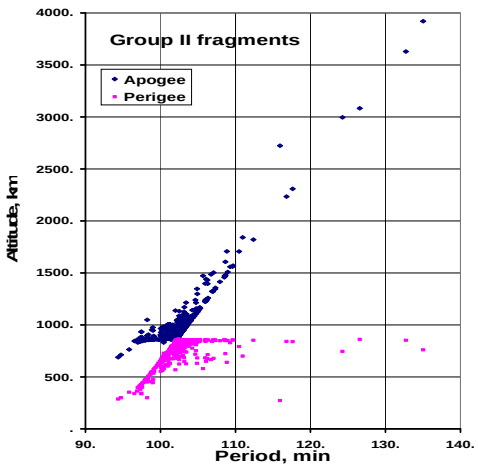

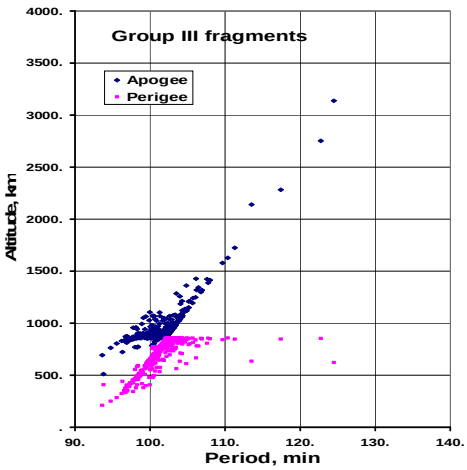

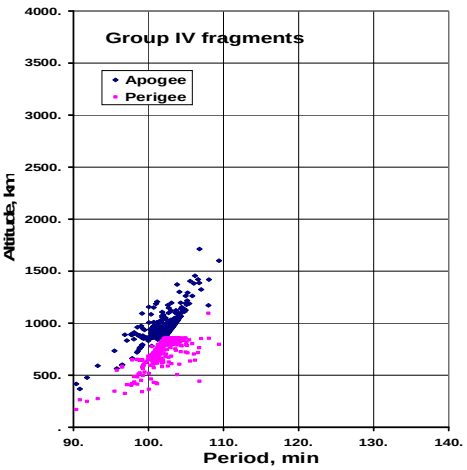

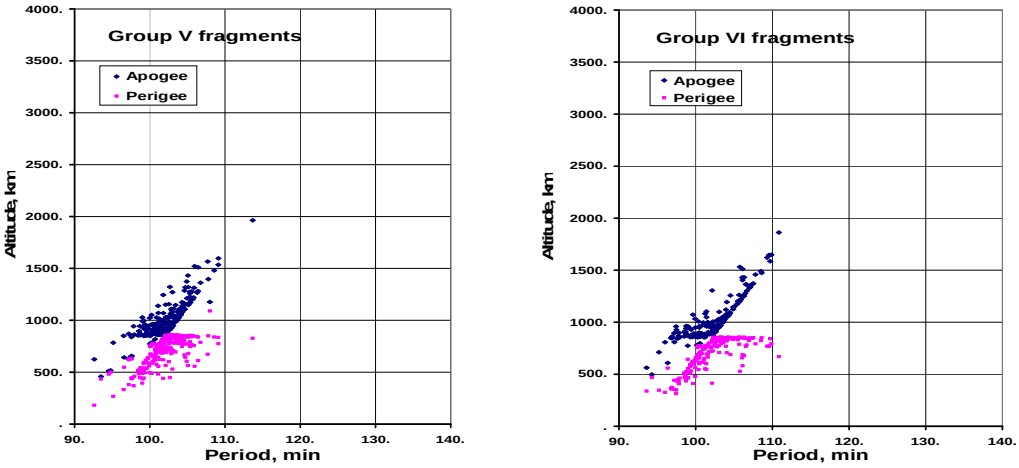

Fig. 1. Gabbard diagrams of groups of fragments of Fengyun-1C fragmentation.

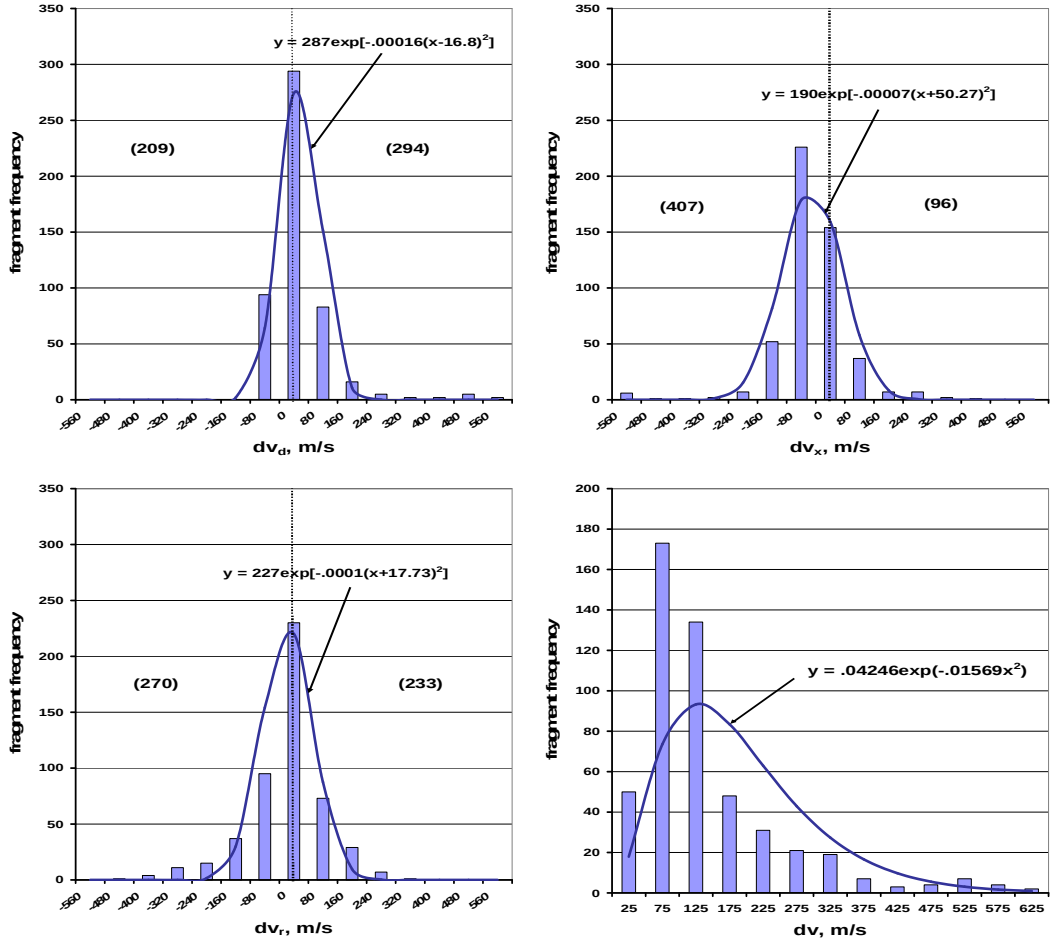

Fig. 2. Frequency distributions of dv_d (upper left), dv_x (upper right), dv_r (lower left) and dv (lower right) of Group I fragments with their corresponding distribution functions. The numbers of fragments in the positive and negative directions are marked.

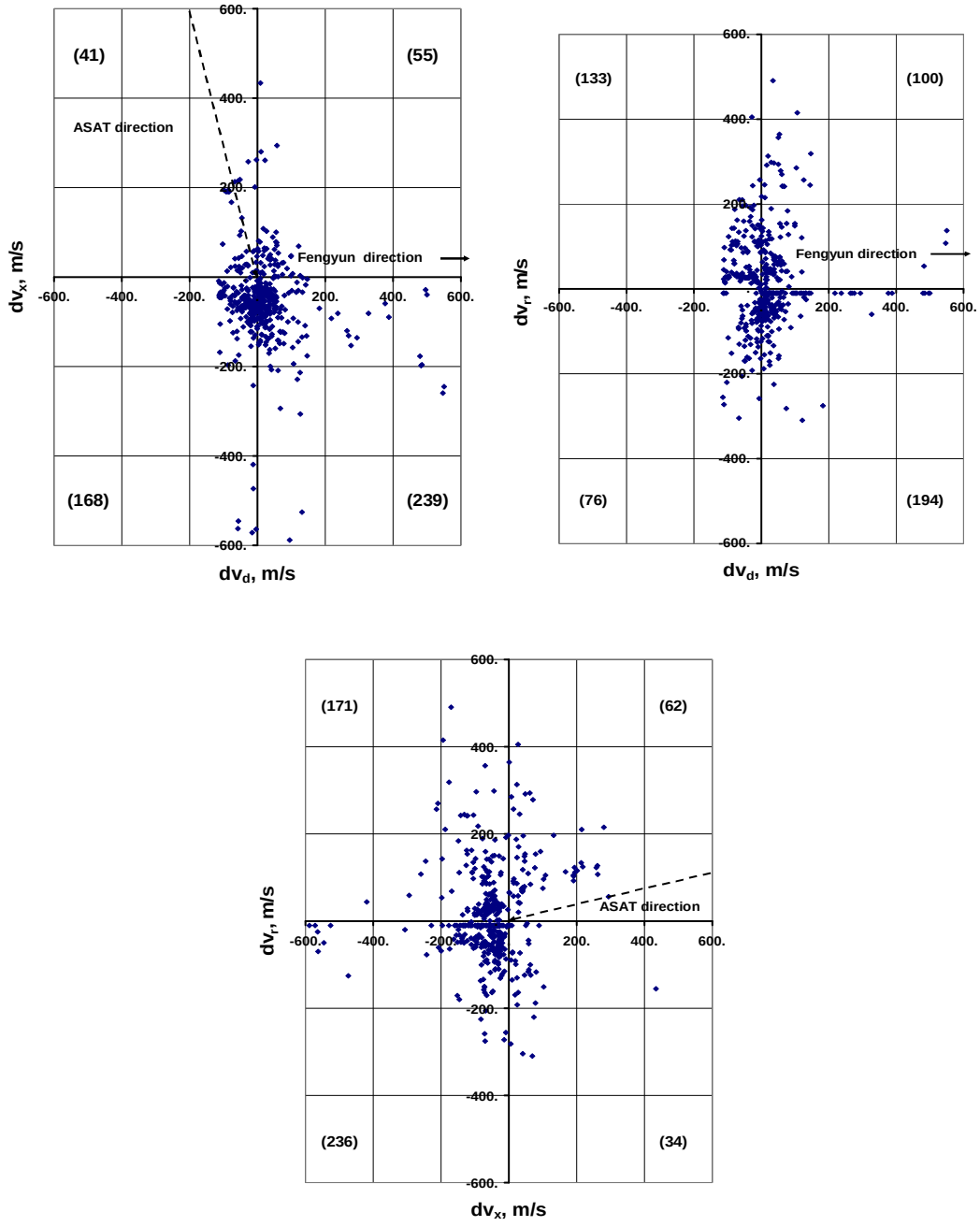

Fig. 3. Scatter-plots of the velocity perturbations components of the Group I fragments in the horizontal plane (upper); a vertical plane containing the momentum of the parent (lower left); and a vertical plane containing the orbital angular momentum of the parent (lower right). The numbers of fragments in each quadrant are marked as well as the approximate directions of the ASAT and its target.

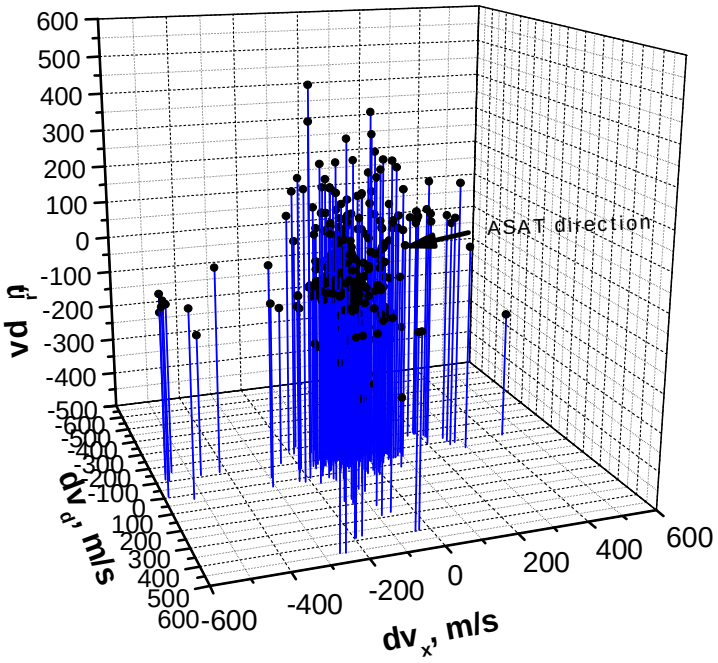

Fig. 4. Three-dimensional scatter-plot of the velocity perturbations components of the Group I fragments in the radial, down-range and cross-range directions in the parent satellite's frame of reference at fragmentation. The approximate direction of the oncoming ASAT is shown.

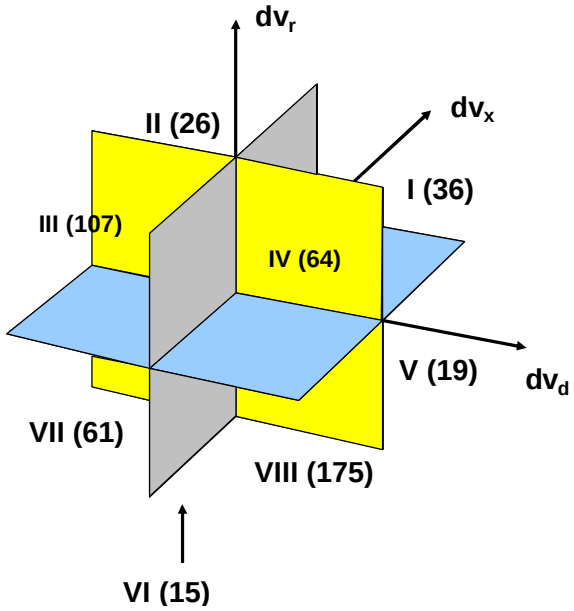

Fig. 5. Fragment counts in octants of space in Fengyun-1C's frame of reference prior to breakup defined by the down-range (dv_d), cross-range (dv_x) and radial (dv_r) directions.

Table I. Mean characteristics of fragments within a Group

	Group I 503 fragments	Group II 439 fragments	Group III 394 fragments	Group IV 343 fragments	Group V 272 fragments	Group VI 191 fragments
Mean i', deg	98.9599	99.0003	98.9799	98.9108	98.8906	98.8607
Mean e'	.0195821	.0186998	.0163063	.0150397	.0170449	.0214641
Mean a', km	7272.97	7259.09	7223.34	7219.99	7227.58	7235.45
Mean P', min	102.91	102.61	101.84	101.77	101.93	102.10
Mean h_a, km	1040.18	1018.83	963.62	950.53	973.07	1013.32
Mean h_p, km	749.46	743.07	726.78	733.16	725.80	701.30
Mean dv_r, m/s	–17.73	–30.82	–3.27	–13.84	–15.88	–17.68
Mean dv_d, m/s	16.80	10.08	–6.98	–8.52	–6.10	–2.09
Mean dv_x, m/s	–50.27	–56.61	–53.14	–42.33	–39.21	–34.38
Mean dv, m/s	143.01	133.07	126.72	142.69	177.07	171.80

DISCUSSION

There are many similarities between the Chinese ASAT experiment of 2007 and the U.S. ASAT experiment 22 years earlier. Both were aimed at functioning satellites in orbit and both used kinetic kill vehicles launched from space facilities nearby. In both cases, the ASAT hit its target from generally sideways and from slightly above the local horizontal plane. Both target satellites were of comparable masses, Fengyun-1C (950 kg) being slightly heavier than Solwind P78-1 (850 kg). The major difference was in the intensities of the fragmentations with the Chinese experiment creating far more fragments. One reason could be that the ASAT hit Solwind at a slightly glancing angle [9]. Another important difference is that the Fengyun fragmentation occurred at a higher altitude (860 km versus 525 km). Consequently the fragments created will remain in orbit for years to come and pose danger to functioning spacecraft and future space missions. This issue has been discussed elsewhere [3, 16]. Hopefully, experiments like this will not be repeated in the future.

REFERENCES

[1] Covault, C., Aviation Week and Space Technology, 17 January 2007.
[2] History of On-orbit Satellite Fragmentation, 14th Ed., NASA Johnson Space Center, 2008, p.386.
[3] Neuneck, G., The Yearbook on Space Policy, Vol. 1, 2008, pp. 211-224.
[4] Aviation Week and Space Technology, September 1985, pp. 20, 21.
[5] Wang, T. "Analysis if Debris from the Collision of the Cosmos 2251 and the Iridium 33 Satellites, " Science & Global Security, Vol. 18, 2010, pp. 87-118.
[6] Orbital Debris Quarterly News, Vol. 17, Issue 1, 2013, pp. 4-5.
[7] https://www.space-track.org/perl/id_query.pl.

[8] Badhwar, G.D., Tan, A., and Reynolds, R.C. “Velocity Perturbations Distributions in the Breakup of Artificial Satellites, ” Journal of Spacecraft and Rockets, Vol. 27, 1990, pp. 299-305.
[9] Tan, A., Badhwar, G.D., Allahdadi, F.A., and Medina, D.F. “Analysis of the Solwind Fragmentation Event Using Theory and Computations, ” Journal of Spacecraft and Rockets, Vol. 33, 1996, pp. 79-85.
[10] Tan, A. and Zhang, D. “Analysis and Interpretation of the Delta 180 Collision Experiment in Space, ” The Journal of the Astronautical Sciences, Vol. 49, 2001, pp. 585-599.
[11] Tan, A. and Ramachandran, R. “Velocity Perturbations Analysis of the Spot 1 Ariane Rocket Fragmentation, ” The Journal of the Astronautical Sciences, Vol. 53, 2005, pp. 39-50.
[12] Tan, A., Zhang, T.X., and Dokhanian, M. “Analysis of the Iridium 33 and Cosmos 2251 Collision Using Velocity Perturbations of the Fragments, ” Adv. Aerospace Sci. and Applications, Vol. 3, 2013, pp. 13-25.
[13] Tan, A. “Ricochet Fragments: A Sufficient Condition for Collision in Space?, ” Orbital Debris Monitor, Vol. 9, 1966, pp. 4-7.
[14] King-Hele, D. Theory of Satellite Orbits in an Atmosphere, Butterwrths, London, 1964, p. 4.
[15] Johnson, N.L., Stansbury, E., Liou, J.C., Hortsman, M. Stokely, C., and Whitlock, D. “The Characteristics and Consequences of the Break-up of the Fengyun-1C Spacecraft, ” Acta Astronautica, Vol. 63, 2008, pp. 128-135.
[16] Kelso, T.S. “Analysis of the 2007 Chinese ASAT Test and the Impact on the Space Environment, ” 2007 AMOS Conference, Maui, Hawaii, pp. 321-330.